Proceedings of the ASME 2019 14th International Manufacturing Science and Engineering Conference
MSEC2019
June 10-14, 2019, Erie, PA, USA

MSEC2019-2816

ULTRASONICALLY-INDUCED PATTERNING OF VIABLE CELLS IN VISCOUS BIOINKS DURING 3D BIOFABRICATION

Parth Chansoria
Edward P. Fitts Department of Industrial and Systems Engineering, North Carolina State University, Raleigh, NC 27695, US

Comparative Medicine Institute, North Carolina State University, Raleigh, NC 27695, US

Rohan Shirwaiker[1]
Edward P. Fitts Department of Industrial and Systems Engineering, North Carolina State University, Raleigh, NC 27695, US

Comparative Medicine Institute, North Carolina State University, Raleigh, NC 27695, US

Joint Department of Biomedical Engineering, North Carolina State University and University of North Carolina at Chapel Hill, Raleigh, NC 27695, US

ABSTRACT

In attempts to engineer human tissues in the lab, bio-mimicking the cellular arrangement of natural tissues is critical to achieve the required biological and mechanical form and function. Although biofabrication employing cellular bioinks continues to evolve as a promising solution over polymer scaffold based techniques in creating complex multi-cellular tissues, the ability of most current biofabrication processes to mimic the requisite cellular arrangement is limited. In this study, we propose a novel biofabrication approach that uses forces generated by bulk standing acoustic waves (BSAW) to non-deleteriously align cells within viscous bioinks. We computationally determine the acoustic pressure pattern generated by BSAW and experimentally map the effects of BSAW frequency (0.71, 1, 1.5, 2 MHz) on the linear arrangement of two types of human cells (adipose-derived stem cells and MG63) in alginate. Computational results indicate a non-linear relationship between frequency and acoustic pressure amplitude. Experimental results demonstrate that the spacing between adjacent strands of aligned cells is affected by frequency ($p < 0.0001$), and this effect is independent of the cell type. Lastly, we demonstrate a synergistic technique of gradual crosslinking in tandem with the BSAW-induced alignment to entrap cells within crosslinked hydrogels. This study represents an advancement in engineered tissue biofabrication aimed at bio-mimicry.

Keywords: biomimicry, bulk standing acoustic wave, ultrasound, anisotropy, biofabrication, pressure nodes, alginate, human adipose-derived stem cells, human osteosarcoma cells.

NOMENCLATURE

r	cell radius (m)
P_0	pressure amplitude (Pa)
k_c	compressibility of the cell (Pa^{-1})
k_s	compressibility of the bioink solution (Pa^{-1})
η	dynamic viscosity of of bioink solution (cP)
c	speed of sound in fluid medium (m/s)
f	frequency of ultrasound (MHz)
k	wave number = $2\pi f/c$ (m^{-1})
L_c	distance between piezo plate and reflector (m)
v	instantaneous velocity of the cell (m/s)

INTRODUCTION

Most eukaryotic tissues have an intrinsic anisotropy in the distribution of cellular and extracellular components that plays a role in their biological and biomechanical functions [1,2]. For example, the striated tubular fibers in Balsa wood enable nutrient transport through capillary action, whilst providing high bending strength and torsional stiffness [3]. A similar arrangement of linearly aligned collagenous fibers is found in human ligaments and tendons [4,5], and it contributes to their ability to transmit tensile loads experienced at the joints. Current efforts in tissue engineering and regenerative medicine (TERM) to create lab-grown tissues and organs that bio-mimic the microarchitecture of human tissues try to do so by first aligning the cells, which then produce aligned extracellular matrix (ECM). This has been extensively investigated at different micro and nano length

[1] Contact author: rashirwaiker@ncsu.edu

scales using electrospun and 3D-printed scaffolds with aligned polymer fiber architectures [6,7]. Herein contact guidance through the physical cues or architecture of the polymer fibers guide ECM formation from the cells.

Recently, 3D biofabrication approaches have gained increased interest owing to their capability in achieving high cell seeding efficiency and multiplicity of cell types [8–10]. However, a homogeneity of cell distribution in the constitutive bioinks and absence of polymer fibers for contact guidance results in non-aligned ECM within biofabricated constructs during maturation. Recent investigations concerning high cell densities along narrow hydrogel (crosslinked bioink) strands have shown that cell-cell signaling can supplant the physical cues needed to produce aligned ECM [11,12]. Thus, a biofabrication approach that could non-deleteriously align the cells across one or more layers of crosslinked hydrogel would further TERM advances towards bio-mimicking engineered tissues. Accordingly, a non-contact approach of ultrasonically guided cellular alignment is proposed herein as a promising solution.

In this study, we investigate the ability of bulk standing acoustic wave (BSAW) with ultrasonic frequency to modulate alignment of cells within a viscous bioink solution. The process uses a novel fixture consisting of a piezo ceramic plate transducer opposite to a reflective surface to arrange cells along linear trajectories within the hydrogels. Demonstration of alignment in multiple cell types (human adipose-derived stem cells (hASC) and human osteosarcoma cells (MG63)) with varying morphology and size in alginate, a commonly used tissue engineering hydrogel, is assertive of the scalability of this approach in terms of creating anisotropic engineered tissues.

APPARATUS AND PROCEDURE

BSAW fixture and mechanism of ultrasonically generating cellular alignment

The BSAW fixture developed for studying the cellular alignment is shown in figure 1. It consists of a piezo-ceramic plate (SM 111, Steiner & Martins Inc) and an opposing glass reflector attached to a cuboid 3D printed out of ABS (uPrint SE Plus, Stratasys). During biofabrication, the fixture is filled with PBS and the bioink is subsequently added and the piezo plate vibrated using a sinusoidal voltage signal generated from a function generator (Keysight Technologies Inc.) and amplified from an RF amplifier (Electronics & Innovation Ltd.). The frequency of oscillation of the signal is the resonant frequency in thickness mode of vibration for the piezo-plates. The resultant vibration creates a longitudinal bulk acoustic wave in the fluid. The interference of this wave with its reflection from the opposing reflector creates a bulk standing acoustic wave (BSAW) with pressure varying only along the x-axis, given by:

$$p(x,t)=P_0\cos(2\pi ft)\cos(kx) \quad (1)$$

where P_0 is the pressure amplitude, f is the ultrasonic frequency and k is the wavenumber ($2\pi f/c$). The nodes of this pressure variation are planes parallel to the transducer-reflector surfaces and are spaced out by $\lambda/2$, where λ is the ultrasound wavelength (c/f). Equation (1) is followed up with a boundary condition given by:

$$L_c = n\lambda/2 \quad (2)$$

where L_c is the critical distance between transducer and reflector surfaces and n is an integer. This imposes a design constraint on the fixture, wherein L_c needs to be an integer multiple of half of the ultrasound wavelength for a standing wave to exist. For speed of sound in water (c) at 1500 m/s, a distance of 42 mm suffices the design constraint for the four frequencies that will be computationally and investigated in this study. Now, on the suspended cells in the bioink, due to the presence of the standing wave, acoustic radiation force (ARF) imposed upon the cells aligns them at the nearest nodes. This force is given by:

$$ARF = (\pi/3)(k_s-k_c)r^3kP_0^2\sin(2\pi x/\lambda) \quad (3)$$

where k_s and k_c are the compressibility of bioink solution and cell, respectively, and r is the cell radius. From equation (3), it is evident that the ARF would increase by increasing the frequency, pressure amplitude, and the radius of the cell. Pertaining to the variable cell radius and frequency in the study, a signal voltage amplitude of 64 Vpp applied to the piezo-ceramic plate generates sufficient pressures and associated ARF at each frequency for each cell type to create well-defined cellular strands within 1 min of actuation time.

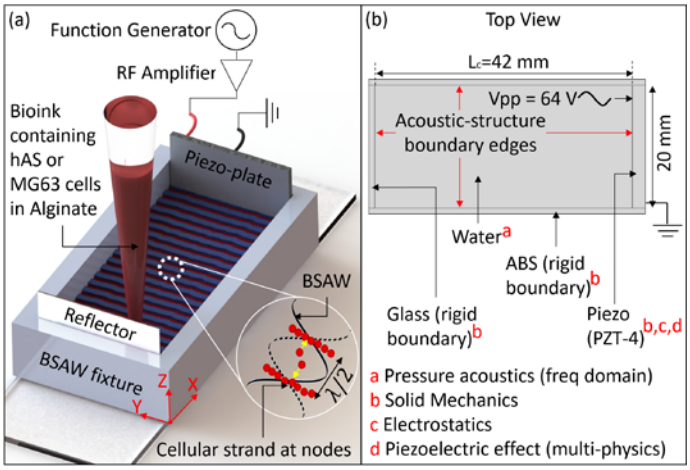

Figure 1. (a) BSAW fixture for aligning cells in viscous bioinks. The BSAW pressure distribution (inset) exerts radiation force on the cells to arrange them along straight cellular strands. (b) 2D linear acoustic model of the top view fixture depicting the multiphysics interfaces in COMSOL.

Computational model in COMSOL to determine acoustic pressure variation

As per theory, the planar BSAW pressure nodes would appear as straight lines in the top view of the fixture. A 2D linear

acoustic finite element analysis (FEA) model was thus setup to determine the pressure variation in top view, which would depict how the corresponding cellular arrangements would emerge and also be indicative of the acoustic pressure amplitudes across the depth of the fluid. The model was formulated in the Acoustic-Piezoelectric interaction interface in COMSOL Multiphysics® (Comsol Inc.), with corresponding interfaces setup as per figure 1(b). Since the fixture was pre-filled with PBS, the liquid between piezo plate and reflector surface was assigned as water with sound attenuation per unit length (dB/m) dependent on frequency [13]. Inbuilt PZT-4 material's properties were utilized within the solid mechanics and electrostatics interfaces. A fixed constraint was assigned to all edges apart from the piezo plate edge in contact with water. To this edge, a harmonic perturbation having voltage amplitude of 32 V was applied, while the other edge was grounded. For the entire model at each frequency (0.71, 1, 1.5, 2 MHz), a free triangular mesh with maximum size of 0.03 mm was used to achieve convergence [14]. The model was computed for four different top-views, each having piezo plate thickness dependent on the resonant frequency as per the manufacturer. On a desktop computer with 32 GB of RAM and 16 GB of dedicated graphics, the computation for each geometry with about 10^6 degrees of freedom lasted nearly 5 minutes.

Bioink preparation

The cell suspensions for the bioink were prepared by plating cryopreserved hASC (R7788115, Thermo Fisher Scientific) or MG63 cells (CRL®-1427™, ATCC) in T-75 flasks (Nunc™ Easy Flask™, Thermo Fisher Scientific) at seeding density of 250,000 cells per flask. The culture media for hASC included MesenPro RS basal media with growth supplement (Thermo Fisher Scientific) and 1% L-Glutamine (Thermo Fisher Scientific). The MG63 cells were cultured in 90% v/v minimum essential medium without L-glutamine (Sigma-Aldrich) and 10% v/v fetal bovine serum (Thermo Fisher Scientific). The flasks were incubated at 37°C and 5% CO_2 with media changes at alternate days until 80% confluency. The live cells in the culture were then selectively stained using neutral red dye (Sigma-Aldrich). For this, the supernatant media in each T-75 flask was replaced with filter-sterilized neutral red media containing 10 mg of dye in 10 ml of relevant growth media depending on the cell type. After incubation in the neutral red media for 1 h, cells were harvested using 0.25% Trypsin-EDTA (Sigma-Aldrich), and a cell pellet was formulated by spinning down the cells at 120 g for 5 min.

For the bioink matrix, 0.6 g of high molecular weight alginate (Manugel® GMB, DuPont) powder was mixed with 29.4 ml of PBS (Sigma-Aldrich) to form a 2% w/v alginate solution. This solution was vortexed for 5 min, sonicated for 1 h, and then autoclaved for 30 min at 121°C and 16 psi (BioClave 16, Benchmark Scientific Inc.) to form the alginate matrix (η ~70 cP). Through gentle pipetting, the cell pellet was homogeneously dispersed in this matrix at 1 million cells/ml to formulate the bioink.

Capturing and analyzing the microarchitecture of cellular alignment in alginate

Three separate BSAW fixtures were made at each frequency to align the cells and measure characteristics of alignment. During the study, the fixtures were placed underneath the stage of a dissection microscope (EZ4 D, Leica Microsystems), and 4 ml of PBS added into the fixtures followed by adding 1 ml of the bioink near the reflector resulting in a 1.2 mm thick construct. Addition of bioink away from the piezo plate shielded the cells from any heat from the piezo plate. The continuous sinusoidal signal was then parsed to the piezo-plate that generated BSAW in the fixture to align the cells. Top view images were captured right before applying the signal and at 30 s and 60 s. In the images captured at 60 s of actuation time, inter-cellular strand spacing was measured in ImageJ [15] by computing the distance between adjacent strands in 3 distinct regions in each image. A two-way ANOVA test, with significance level $\alpha = 0.05$, was then used to determine the significance of the effect of cell type and frequency on the spacing. Tukey's HSD post-hoc tests were used to determine any pair-wise differences.

Lastly, to demonstrate the pertinence of the presented study for tissue engineering applications, the alginate was crosslinked to determine if the alignment was retained within the gelled construct. The crosslinking protocol involved addition of 4 ml of 1% w/v $CaCl_2$ in DI water in the fixture after 1 min of actuation time. Actuation was switched off after 30 min, and the resulting construct was taken out and imaged.

RESULTS

Results of the computational model

The top view of the pressure variation in the BSAW fixture at each frequency is shown in figure 2. The results agree with theory, in that the pressure nodes are straight lines when viewed from the top. The pressure amplitudes in this arrangement followed a non-linear trend with amplitudes in decreasing order for 1.5, 1, 2, and 0.71 MHz, respectively.

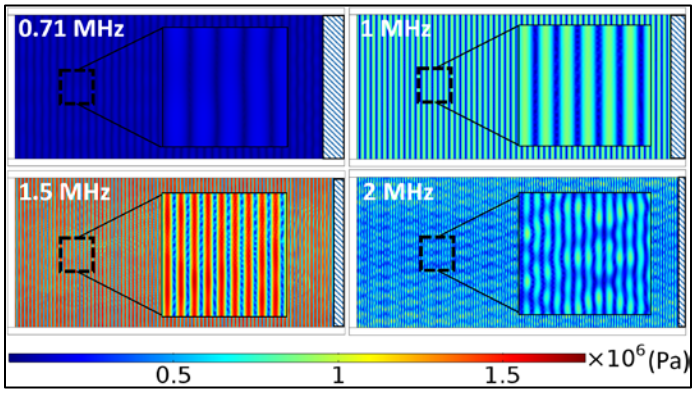

Figure 2. Acoustic pressure distribution in BSAW fixture at each frequency depicting straight pressure node lines as seen from the top. The hatched pattern on the right in each fixture represents the transducer, whose thickness was different at each frequency. The pressure amplitude followed a non-linear trend with the highest amplitude for 1.5 MHz and lowest for 0.71 MHz.

Results of the cellular alignment at varying frequency

As the sinusoidal voltage signal was actuated, the resulting BSAW due to piezo plate vibration slowly aligned the cells at their nearest pressure nodes to form cellular strands. This slow progression of hAS cells alignment is evident in figure 3(b). Although the pressure amplitude at 0.71 MHz was about an order of magnitude less than that at 1.5 MHz, distinct and measurable cellular alignment was still observed after 60 s of actuation. Figure 3 (c-f) depicts the alignment at each frequency after 60 s.

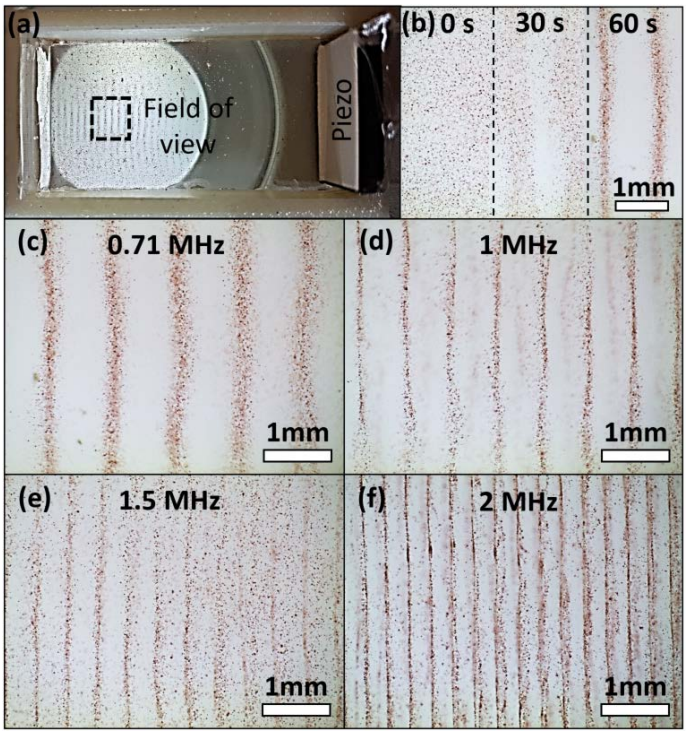

Figure 3. (a) Top view of BSAW fixture at 0.71 MHz. (b) Progression of alignment of hAS cells over time within the 0.71 MHz fixture. (c-f) Strands of hAS cells aligned within alginate using ultrasonic frequencies 0.71, 1, 1.5, and 2 MHz, respectively after 60 s of BSAW actuation. The alignment characteristics of MG63 cells were similar to hAS cells.

Figure 4(a) depicts the measured inter-cellular strand spacing from ImageJ analysis. The two-way ANOVA results denote significant effect of only the frequency ($p < 0.0001$) in governing the spacing, while there is no significance of the main effect of cell type ($p = 0.97$) or their interaction ($p = 0.08$). Post-hoc results indicate that although the spacings at each frequency were independent of the cell type, for both cell types, spacing at each frequency was significantly different ($p < 0.01$). All of the measured spacings are also closely correlated with theoretical spacing, indicative of the predictable controllability of the cellular strands microarchitecture by variation of only the ultrasonic frequency.

Figure 4(b) demonstrates the entrapping of the neutral red stained hASC within crosslinked alginate. The presence of pre-filled PBS in the fixture uniformly dispersed the Ca^{2+} gelation ions, slowly crosslinking the alginate. As crosslinking progressed over 30 min, the continuous excitation of the transducers ensured that the aligned cells remained in position. Since the neutral red dye selectively stains the live cells, exhibition of redness in the cells post construct fabrication is indicative of the non-deleteriousness of the BSAW-assisted alignment.

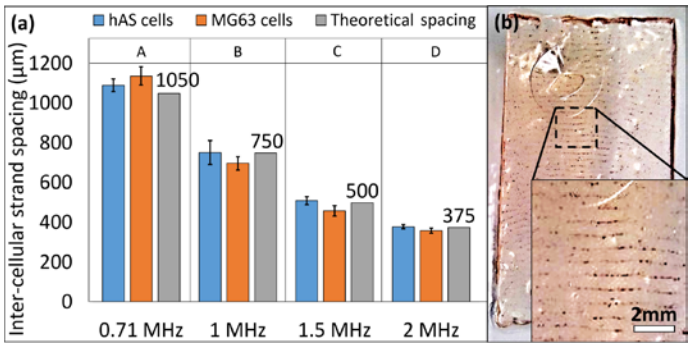

Figure 4. (a) Measured and theoretical inter-cellular strand spacing for hAS and MG63 cells. Results confirm a significant effect of frequency ($p < 0.0001$) on the spacing. The spacing at each frequency and cell type had a close correlation with the theoretical frequency. Letters A-D denote statistically significant post-hoc differences ($p < 0.01$). (b) A crosslinked construct depicting preservation of alignment within chemically crosslinked construct.

DISCUSSION

Building anisotropy in engineered tissues is necessary for capturing the desired form and function of the native tissue. This anisotropy can be induced first and foremost by appropriately arranging cells within the construct. Towards achieving this, the ultrasonic BSAW-assisted approach of rendering cellular alignment, which has potential to promote subsequent ECM production through cell-cell signaling in cellular clusters, seems promising in alleviating the shortcomings of biofabrication approaches in providing contact guidance based alignment. Ultrasound has been widely utilized in medical imaging to non-invasively characterize tissues [16,17]. More recently, ultrasound-based cell manipulation has gained attention to create bio-models [18,19] or chemical assays [20,21] due to the micro-manipulation capability and minimal effect on the physiological properties of cells.

This study has demonstrated how the alignment pattern can be controlled by varying the ultrasonic frequency. Since the neutral red dye should only be retained within live cells, exhibition of red staining within the gelled constructs is indicative of the non-deleteriousness of ultrasound during biofabrication. Future studies will focus on assessing the cell metabolic activity, phenotype and ECM formation in culture over time. Although we have demonstrated alignment in alginate whose viscosity is in the higher ranges for bioink matrices, its polymeric chains lag the ligands necessary for cell attachment and subsequent ECM production. As such, peptide modifications

of alginate [22,23] or other adherent biopolymers [24] could be sought for extended maturation of the constructs in future. Changing the bioink (more specifically, the bioink viscosity) would necessitate the re-optimization of process parameters and crosslinking protocol to entrap the cellular patterns within the biofabricated construct. For viscous bioinks, a cell migrating to the nearest node due to the ARF would be slowed down by viscous drag force (DF) from the bioink, given by:

$$DF = 6\pi\eta rv \quad (4)$$

where η is the dynamic viscosity of the bioink and v is the instantaneous velocity of the cell. In this case, higher voltage amplitude could potentially increase the pressure amplitude, thereby increasing the ARF (equation 3) to achieve quicker alignment. At increased voltage however, greater straining of the transducer might induce undesired turbulence due to acoustic streaming and distort the alignment. Herein, lower voltages coupled with a slow crosslinking protocol similar to the one described in this study could alleviate the streaming issue while achieving cellular alignment. Altering the voltage amplitude would not affect the spacing between adjacent cellular strands as it is only dependent on the wavelength. Changing bioink however, might change the spacing due to different speed of sound at the same frequency. As such, a thorough understanding and optimization of the material and process parameters is required to achieve high fidelity of cellular alignment in the biofabricated constructs relevant to the tissue application.

The approach described in this study has the ability to be integrated with various 3D bioprinting processes including extrusion-based, DLP, SLA, or inkjet ones. Furthermore, the alignment patterns could be altered across the layers by utilizing fixtures with multiple piezo-reflector pairs with different orientations. For example, an orthogonal cellular alignment across two layers could be created by using orthogonal piezo-reflector pairs, wherein the second pair is actuated after the first layer has finished crosslinking. We plan to investigate this approach to create complex architecture across multi-layered tissues. Also, catering to specific tissue types, by varying the frequency and cellular concentration we plan to create cell clusters with varied inter-cellular strand spacing and cell concentration in order to evaluate variation of the modalities that would lead to most functionally relevant ECM production.

CONCLUSION

This study demonstrated a fundamentally new process that utilizes ultrasound to align cells within viscous bioinks. We explained the design principles of a fixture containing a piezo ceramic plate that is vibrated at an ultrasonic frequency to generate standing waves in the bioink which cause the cells to align. The computational model depicted the acoustic pressure variations in the fixture as a pattern of parallel nodal and antinodal lines. The experimental studies showed that the cells clustered along straight lines in accordance with the computational estimations. Furthermore, the spacing between the cellular strands was found to be primarily dependent on the frequency, irrespective of the cell types tested. The neutral red dye expression after biofabrication of chemically crosslinked construct with ultrasonic actuation duration of up to 30 min demonstrated the non-deleteriousness of this process. More comprehensive viability and proliferation assays for extended growth periods of such constructs are still warranted, which our future studies shall focus upon. Other future studies shall entail assessment of ECM production characteristics of aligned cellular strands in response to variations in inter-cellular strand spacing and cellular densities.

ACKNOWLEDGEMENTS

This work was supported by grants from the US NSF (CMMI#1652489) and NVIDIA (GPU grant). We would also like to note that there is a patent pending on the technology described in this paper (US 62747789).

REFERENCES

[1] Bourget, J.-M., A., F., Guillemette, M., Veres, T., and Germain, L., 2013, "Alignment of Cells and Extracellular Matrix Within Tissue- Engineered Substitutes," *Advances in Biomaterials Science and Biomedical Applications*, InTech, pp. 365–390.

[2] Mauck, R. L., Baker, B. M., Nerurkar, N. L., Burdick, J. A., Li, W.-J., Tuan, R. S., and Elliott, D. M., 2009, "Engineering on the Straight and Narrow: The Mechanics of Nanofibrous Assemblies for Fiber-Reinforced Tissue Regeneration," Tissue Eng. Part B Rev., **15**(2), pp. 171–193.

[3] Gibson, L. J., 2012, "The Hierarchical Structure and Mechanics of Plant Materials.," J. R. Soc. Interface, **9**(76), pp. 2749–66.

[4] Kjær, M., 2004, "Role of Extracellular Matrix in Adaptation of Tendon and Skeletal Muscle to Mechanical Loading," Physiol. Rev., **84**(2), pp. 649–698.

[5] Birch, H. L., Thorpe, C. T., and Rumian, A. P., 2013, "Specialisation of Extracellular Matrix for Function in Tendons and Ligaments.," Muscles. Ligaments Tendons J., **3**(1), pp. 12–22.

[6] Warren, P. B., Huebner, P., Spang, J. T., Shirwaiker, R. A., and Fisher, M. B., 2017, "Engineering 3D-Bioplotted Scaffolds to Induce Aligned Extracellular Matrix Deposition for Musculoskeletal Soft Tissue Replacement," Connect. Tissue Res., **58**(3–4), pp. 342–354.

[7] Lee, C. H., Shin, H. J., Cho, I. H., Kang, Y.-M., Kim, I. A., Park, K.-D., and Shin, J.-W., 2005, "Nanofiber Alignment and Direction of Mechanical Strain Affect the ECM Production of Human ACL Fibroblast," Biomaterials, **26**(11), pp. 1261–1270.

[8] Starly, B., and Shirwaiker, R. A., 2015, *Three-Dimensional Bioprinting. Chapter 3 in 3D Bioprinting and Nanotechnology in Tissue Engineering and Regenerative Medicine, Eds. L. Zhang, J. P. Fisher, and*

K. Leong, Academic Press, Waltham, MA.

[9] Narayanan, L. K., Huebner, P., Fisher, M. B., Spang, J. T., Starly, B., Shirwaiker, R. A., and Fitts, E. P., 2016, "3D-Bioprinting of Polylactic Acid (PLA) Nanofiber−Alginate Hydrogel Bioink Containing Human Adipose-Derived Stem Cells," ACS Biomater. Sci. Eng., **2**(10), pp. 1732–1742.

[10] Patra, S., and Young, V., 2016, "A Review of 3D Printing Techniques and the Future in Biofabrication of Bioprinted Tissue," Cell Biochem. Biophys., **74**(2), pp. 93–98.

[11] Aubin, H., Nichol, J. W., Hutson, C. B., Bae, H., Sieminski, A. L., Cropek, D. M., Akhyari, P., and Khademhosseini, A., 2010, "Directed 3D Cell Alignment and Elongation in Microengineered Hydrogels," Biomaterials, **31**(27), pp. 6941–6951.

[12] Kim, S. H., Turnbull, J., and Guimond, S., 2011, "Extracellular Matrix and Cell Signalling: The Dynamic Cooperation of Integrin, Proteoglycan and Growth Factor Receptor," J. Endocrinol., **209**(2), pp. 139–151.

[13] Slotwinski, J., 2002, "Ultrasonics Testing," *Handbook of Reference Data for Nondestructive Testing*, L. Mordfin, ed., ASTM International, pp. 31–48.

[14] Scholz, M.-S., Drinkwater, B. W., Llewellyn-Jones, T. M., and Trask, R. S., 2015, "Counterpropagating Wave Acoustic Particle Manipulation Device for the Effective Manufacture of Composite Materials," IEEE Trans. Ultrason. Ferroelectr. Freq. Control, **62**(10), pp. 1845–1855.

[15] Schindelin, J., Arganda-Carreras, I., Frise, E., Kaynig, V., Longair, M., Pietzsch, T., Preibisch, S., Rueden, C., Saalfeld, S., Schmid, B., Tinevez, J.-Y., White, D. J., Hartenstein, V., Eliceiri, K., Tomancak, P., and Cardona, A., 2012, "Fiji: An Open-Source Platform for Biological-Image Analysis," Nat. Methods, **9**(7), pp. 676–682.

[16] Hunt, J. W., Arditi, M., and Foster, F. S., 1983, "Ultrasound Transducers for Pulse-Echo Medical Imaging," IEEE Trans. Biomed. Eng., **BME-30**(8), pp. 453–481.

[17] Ritter, T. A., Shrout, T. R., Tutwiler, R., and Shung, K. K., 2002, "A 30-MHz Piezo-Composite Ultrasound Array for Medical Imaging Applications," IEEE Trans. Ultrason. Ferroelectr. Freq. Control, **49**(2), pp. 217–230.

[18] D'Urso, P. S., and Thompson, R. G., 1998, "Fetal Biomodelling," Aust. New Zeal. J. Obstet. Gynaecol., **38**(2), pp. 205–207.

[19] Ma, X., Wu, X., Wu, Y., Liu, J., and Sun, L., 2010, "Use of Advanced Computer-Aided Biomodels in Practical Orthopaedic Education," *2010 International Conference on Educational and Network Technology*, IEEE, pp. 120–123.

[20] Viola, F., Mauldin, F. W., Lin-Schmidt, X., Haverstick, D. M., Lawrence, M. B., and Walker, W. F., 2010, "A Novel Ultrasound-Based Method to Evaluate Hemostatic Function of Whole Blood," Clin. Chim. Acta, **411**(1–2), pp. 106–113.

[21] Iloeje, U. H., Yang, H., Su, J., Jen, C., You, S., and Chen, C., 2006, "Predicting Cirrhosis Risk Based on the Level of Circulating Hepatitis B Viral Load," Gastroenterology, **130**(3), pp. 678–686.

[22] Yu, J., Du, K. T., Fang, Q., Gu, Y., Mihardja, S. S., Sievers, R. E., Wu, J. C., and Lee, R. J., 2010, "The Use of Human Mesenchymal Stem Cells Encapsulated in RGD Modified Alginate Microspheres in the Repair of Myocardial Infarction in the Rat," Biomaterials, **31**(27), pp. 7012–7020.

[23] Shachar, M., Tsur-Gang, O., Dvir, T., Leor, J., and Cohen, S., 2011, "The Effect of Immobilized RGD Peptide in Alginate Scaffolds on Cardiac Tissue Engineering," Acta Biomater., **7**(1), pp. 152–162.

[24] Nakamura, M., Iwanaga, S., Henmi, C., Arai, K., and Nishiyama, Y., 2010, "Biomatrices and Biomaterials for Future Developments of Bioprinting and Biofabrication," Biofabrication, **2**(1), p. 014110.